CSIRO PUBLISHING

www.publish.csiro.au/journals/ijwf *International Journal of Wildland Fire*, 2005, **14**, 37–48

Modeling interactions between fire and atmosphere in discrete element fuel beds

Rodman Linn[A,D], *Judith Winterkamp*[A], *Jonah J. Colman*[A], *Carleton Edminster*[B] *and John D. Bailey*[C]

[A]Earth and Environmental Sciences Division, Los Alamos National Laboratory, Los Alamos, NM 87545, USA.
[B]USDA Forest Service, Rocky Mountain Research Station, 2500 S. Pine Knoll Dr., Flagstaff, AZ 86001, USA.
[C]Northern Arizona University School of Forestry, PO Box 15018, Flagstaff, AZ 86011 5018, USA.
[D]Corresponding author. Telephone: +1 505 665 6254; email: rrl@lanl.gov

Abstract. In this text we describe an initial attempt to incorporate discrete porous element fuel beds into the coupled atmosphere–wildfire behavior model HIGRAD/FIRETEC. First we develop conceptual models for use in translating measured tree data (in this case a ponderosa pine forest) into discrete fuel elements. Then data collected at experimental sites near Flagstaff, Arizona are used to create a discontinuous canopy fuel representation in HIGRAD/FIRETEC. Four simulations are presented with different canopy and understory configurations as described in the text. The results are discussed in terms of the same two discrete locations within the canopy for each simulation. The canopy structure had significant effects on the balance between radiative and convective heating in driving the fire and indeed sometimes determined whether a specific tree burned or not. In our simulations the ground fuel density was the determining factor in the overall spread rate of the fire, even when the overstory was involved in the fire. This behavior is well known in the fire meteorology community. In the future, simulations of this type could help land managers to better understand the role of canopy and understory structure in determining fire behavior, and thus help them decide between the different thinning and fuel treatment strategies available to them.

Additional keywords: fire propagation; FIRETEC; HIGRAD.

Introduction

Wildfires comprise a complex set of physical and chemical processes, some of whose interactions depend on the coupling between atmospheric flows, the fire and the vegetation structure. This coupling affects many aspects of the wildfire, such as the balances between different modes of heat transfer, the turbulent mixing which brings gaseous reactants together, and the shape of the fire perimeter.

The influence of plant canopies on atmospheric flows is a well-developed field of study. Much of this work has been focused on characterizing either the average effects of the integrated canopy, the turbulent mixing that is induced by the canopy, or the integrated effects of the canopy on the shear layer above the fuel bed (i.e. Brunet *et al*. 1994; Finnigan and Brunet 1995; Shaw *et al*. 1995). Scaling laws have been used to relate the geometry of obstacles that make up a canopy to the boundary layer that they influence. Work by Belcher *et al*. (2003) describes numerous relationships that characterize the integrated effects of arrays of obstacles on net flow and roughness lengths both within and above the obstacles. This work is focused on spatially averaged time-mean flows. A closure scheme for flow around tree structures has recently been developed by Calogine and Sèro-Guillaume (2002). This work uses a fractal porous media model and averaging techniques to generate a tree-like obstruction that acts as an obstacle for air flow in direct numerical simulations. From these simulations a closure model is generated for the Navier-Stokes equations when applied to flow around a tree. This detailed look at flow around and through tree-like structures represents an important step in being able to better simulate airflow through irregular canopies including vegetation of different sizes and shapes.

There has also been a variety of research done on wildfire propagation of a crown fire as described in Albini and Stocks (1986), Rothermel (1991), Van Wagner (1993), Call and Albini (1997) and Cruz *et al*. (2002). In general, much of this research is focused on the gross aspects of fire behavior such as average spread rate and mean fuel consumption as a fire moves through a canopy. These works have provided critical information for operational fire behavior prediction,

 10.1071/WF04043 1049-8001/05/010037

usually based on balances between averaged canopy-scale processes. However, they have not focused on explaining the balances in physical processes at the tree-scale or the manner in which the heterogeneities of canopy structure change these balances.

The ongoing development of the HIGRAD/FIRETEC wildfire modeling system presents a new tool for the investigation of coupled atmosphere–fire–fuel interactions. This modeling framework is composed of an atmospheric model, HIGRAD (Reisner *et al*. 2000*a*), which is designed to capture high gradients in quantities such as temperature and velocity, and a wildfire model, FIRETEC (Linn 1997). FIRETEC is based on conservation of mass, momentum, species and energy. HIGRAD/FIRETEC has been used to examine fire behavior and the interaction between the fire and atmosphere in several idealized simulations, including idealized grass fires and homogenized understory and canopy simulations. These idealized simulations show strong interaction between fire, atmosphere and vegetation structure. The details concerning the formulation of FIRETEC or HIGRAD or their numerical implementation will not be discussed as most of these details can be found in other publications (Linn 1997; Reisner *et al*. 2000*a*, 2000*b*; Linn *et al*. 2002).

Here we describe an initial attempt to incorporate discrete element fuel beds into HIGRAD/FIRETEC. We address questions such as how a fire responds to changes in canopy arrangement or understory fuel load, and how radiative and convective heat transfer work together to determine which trees will burn and which will not. The structure of the vegetation in these simulations is based on individual tree data measured at experimental sites near Flagstaff, Arizona, which have been arranged as a representation of discontinuous canopy vegetation that resembles ponderosa pine forests. These simulations allow us to examine the interaction of wind and fire in discontinuous fuel beds and, more specifically, to investigate the role that the canopy structure plays in such fires.

In this text we introduce some of the conceptual models that we have used to translate the measured tree data into discrete fuel elements that can be employed in FIRETEC. We describe some simulations that have been performed with these discrete fuel elements (we shall refer to the fuel elements as trees even though they are in fact crude representations of trees), and report on some of the output produced by these simulations. Specific results that demonstrate interaction between the fire and the atmosphere are highlighted as an indication of the potential benefits of using HIGRAD/FIRETEC to investigate wildfire behavior in discontinuous canopies.

Fuel representation

HIGRAD/FIRETEC is a finite volume computer program that uses a structured three-dimensional grid to describe evolving, spatially varying quantities such as temperature, the velocity of the gaseous species and various characteristics of the fuel. In its current implementation it cannot represent individual leaves, needles or twigs as done by other researchers using fractal (Calogine and Sèro-Guillaume 2002) or other methods. Instead, the multiphase stochastic approach used in FIRETEC represents vegetation as a porous medium that provides bulk momentum and heat exchange terms between gas and solid phases. Fuel is described by assigning mean or bulk quantities such as fine fuel surface area per unit volume, moisture ratio and density to each cell in the three-dimensional grid. This methodology potentially allows HIGRAD/FIRETEC to simulate complex fuel beds that are vertically and horizontally non-homogeneous. The approach is described in detail in Linn (1997) and has similarities to the multiphase approach used by Morvan and Dupuy (2001).

Researchers from the USDA Forest Service (led by Carleton Edminster) and Northern Arizona University (led by John Bailey) measured canopy vegetation characteristics on several 20 m × 50 m plots near Flagstaff, Arizona. Data were collected for each tree within the plots as a part of the Fire/Fire Surrogate program, which is funded by the Joint Fire Sciences Program with additional funding from the Rocky Mountain Research Station. The data that were collected included tree height, height to live crown, height to dead crown, diameter of the crowns in two directions, and diameter of the trunks at breast height for each tree within the plots.

After this extensive sampling effort, the challenge was to convert the collected data into three-dimensional fuel distributions that could be used in HIGRAD/FIRETEC to simulate a fire burning through trees similar to those measured. For this initial effort, we chose to work with a simple bulk averaged structural model for a ponderosa pine tree. In the future, we hope to explore other structural models in collaboration with other researchers. It was assumed that the majority of the fine fuels form a shell around the outside of the canopy that can be described with paraboloids, and that the density of the fine fuels declines from the outside of the tree to the center of the tree (especially near the bottom of the canopy). We also chose to treat the trees as if they were axisymmetric.

With these ideas in mind, we used a series of parabolic profiles to generate a function that describes the distribution of the mass of an idealized tree as shown in Fig. 1. From these profiles and the locations of the trees, we can establish the bulk density of fine vegetation within each cell of the three-dimensional HIGRAD/FIRETEC mesh. Each cell in the mesh can contain part of one tree, parts of more than one tree, or be in a location where there are no trees.

The first step in resolving each tree is to define the locations that are inside the tree perimeter. The formulation that we used to define the interior of the tree crown is shown in equation (1) in terms of a height above the ground, z, and a

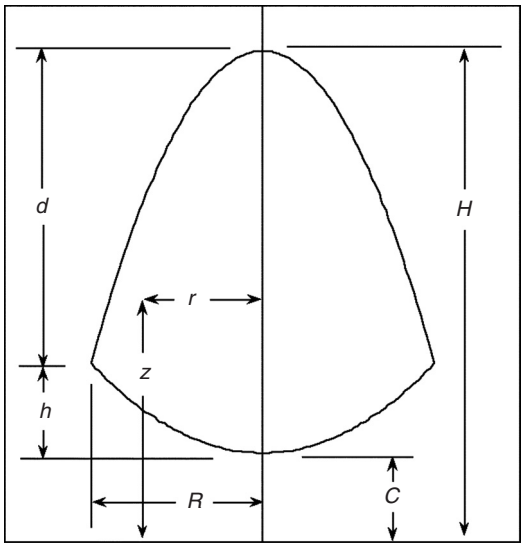

Fig. 1. This diagram shows a two-dimensional cross section of the axisymmetrical three-dimensional shape that we use to describe the crowns of trees in our simulations. The black outline of the tree canopy consisting of two parabolas bounds a region where bulk density is non-homogeneously distributed. A location inside the crown is specified by z and r. C, R and H are specified from the field data.

distance from the center of the particular tree, r:

$$\frac{h}{R^2}[r^2] + C \leq crown_{interior} \leq -\frac{d}{R^2}[r^2] + H. \qquad (1)$$

The variables are illustrated in Fig. 1. The variables h and d are used to scale the parabolic shapes that form the top and bottom of the crown and, when summed, they equal the difference between the height of the tree, H, and the height to crown, C. An estimated value of $h = d/4$ is currently being used based on a limited number of observations. R is the crown radius at its widest point. The density in the interior of the tree, ρ_{canopy}, is approximated by equation (2):

$$\rho_{canopy} = \left[\frac{z - C + \frac{d}{R^2}r^2}{H - C}\right]\rho_{\max}. \qquad (2)$$

By requiring the integral of this function over the interior of the crown to be equal to the volume of the crown multiplied by an average crown bulk density (bulk density of the crown of a single tree), we get the expression in equation (3):

$$\rho_{\max} = \frac{6}{5}\rho_{avg}. \qquad (3)$$

The average crown density for individual trees was chosen to be 0.4 kg/m^3 based on discussions with forestry researchers. These expressions provide a method for converting standard tree canopy measurements for ponderosa pine trees into a spatial distribution of vegetation bulk density suitable for use in HIGRAD/FIRETEC.

Fig. 2. A cut-away cross-section of a portion of the fuel bed used in the patches simulation. The image shows an isosurface of fuel density at a value of 0.3 kg/m^3 looking across a section roughly 100 m × 100 m × 20 m.

Because the sampled plots were only 20 m × 50 m in size and we wished to simulate fires over much larger regions, we chose to distribute the trees randomly in several adjacent 20 m × 50 m domains. This methodology allows us to generate large stands of trees without having the periodic arrangement that would occur if we used the same locations for the trees within each 20 m × 50 m plot.

The analytical expressions in equations (2) and (3) describe the distributions of bulk density within the canopy volume outlined by equation (1). Because most of the trees in the database are between 10 and 18 m tall and between 2 and 6 m in diameter, the trees will at least partially occupy multiple computational cells that have horizontal dimensions of 2 m and vertical dimensions of ~1.5 m near the ground. In order to use the idealized trees described above, we must convert the analytically described, continuously varying fuel distributions into discrete values that represent average bulk properties for each cell that contains part of a tree. This is done by numerically integrating the density over the volume of canopy that lies within each cell (as defined by the tree's geometrical data and location) and dividing it by the cell volume as described in equation (4):

$$\overline{\rho} = \frac{\int_{cell\ volume} \rho_{canopy} dv}{cell\ volume}. \qquad (4)$$

Figure 2 displays a cut-away cross section of a fuel bed that was generated using the methodology described above. In Fig. 2, many different sizes and shapes of trees are illustrated by drawing an isosurface at the locations where the bulk density of the vegetation was 0.3 kg/m^3.

The current model for ground fuel includes a load for grass and a load for litter. We make the assumption that the amount of grass fuel falls off as a function of the mass of canopy above it, normalized by the maximum expected mass for the average tree canopy depth, s, while the litter load increases as a function of the amount of canopy above it. This model is described by equation (5), in which m_{ground} is the mass per square meter of the combined grass and litter, m_{grass} is the mass per square meter of the grass in the lowest cell when there is no canopy above it, m_{litter} is a assumed maximum litter mass per square meter on the ground under maximum canopy cover, and c_g and c_l are non-dimensional proportionality constants.

$$m_{ground} = m_{grass}e^{-c_g s} + m_{litter}(1 - e^{-c_l s}). \qquad (5)$$

The values of m_{grass}, m_{litter}, c_g and c_l, decided in consultation with forest service researchers, were chosen to be 0.7 kg/m^2, 33 kg/m^2, 5 kg and 5 kg respectively for the set of simulations described in this text. It should be noted that the litter density almost never gets above 0.25 as s seldom reaches 1.0. The bulk density of ground fuels is added to any bulk density that low canopy might contribute to that cell. One trait of this representation of the fuel is that the size of the grid cells can greatly affect the bulk density of the fuel in the cell but does not change the mass of the fuel in the cell that is available to burn.

Simulations

Some specific questions that arise when trying to examine wildfire responses to fuel arrangement and structure are:

1. Does the distribution of tree shapes and sizes within a canopy change the likelihood of a particular tree being burned?
2. Does the position of a tree within a canopy change the likelihood of that specific tree being burned?
3. Is the canopy structure the most important factor in determining spread rate or is the speed of the ground fire a critical factor?

We performed four simulations with different canopy and understory configurations. In each of the simulations we ignited a fire near a 60 m wide fuel break (area with no fuel). The fuel break was included to eliminate the effects of variations in canopy structures upwind of the ignition location. The fire was blown with a 6 m/s wind across a 20 m grass area toward a forested region. The forested region was 220 m wide, with a 20 m area of grass on the far side of the forest. The total horizontal domain of the simulations was 320 m × 320 m, including the forest, the grasslands and the fuel break. The horizontal resolution near the ground was 2 m, and the vertical resolution was ~1.5 m at the ground. The FIRETEC time step in these simulations was 0.002 s. The simulations were allowed to continue until the fire neared the boundary of the mesh (150–220 s after ignition).

In the first simulation, which we will refer to as the 'full' forest simulation, the canopy was created using the methodology described above over a 220 m × 320 m region. This simulation is depicted in Fig. 3. The canopy in this simulation consisted of over 5000 trees. The canopy bulk density over the forested region was ~0.24 kg/m^3.

The forest canopy in the second simulation was derived from the canopy in the first simulation by removing every tree that had a trunk diameter of less than 28 cm at breast height. Trunk diameter was one piece of the field data that was collected for each tree. The diameter threshold was chosen arbitrarily for testing purposes, but is a variable often employed in thinning strategies. An image from this simulation is shown in Fig. 4. There were only about 1000 trees in this forested area. The canopy bulk density over the forested region was ~0.055 kg/m^3. We will refer to this simulation as the 'thin' simulation for the rest of the text.

The third simulation, hereafter called the 'patches' simulation, contained a canopy derived from that used in the full forest case. In this simulation, trees were removed to leave patches of varying-sized trees. The patches were placed arbitrarily, with the mean spacing between patches in the order of 50 m and the average radius of the patches ~15 m. An image from this simulation is shown in Fig. 5. The canopy bulk density over the forested region was ~0.066 kg m^{-3}.

The canopy used in the fourth simulation is the same as the canopy in the patches simulation, but the grass in the understory has been cut in half (by reducing both the height and mass of the fuel). An image from this simulation is shown in Fig. 6. We refer to this simulation as the 'patches, less ground fuel' (PLGF) simulation. The four simulations are summarized in Table 1.

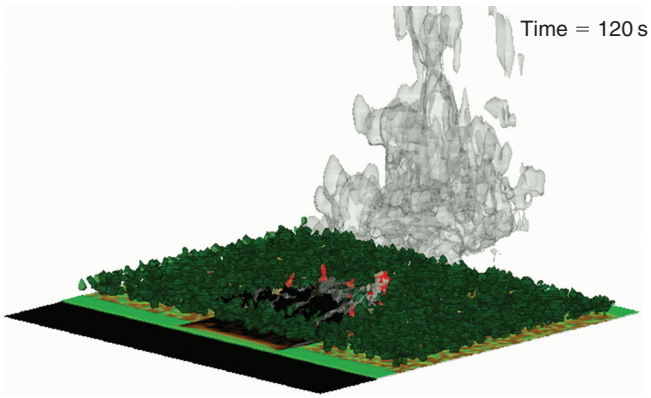

Fig. 3. Image from the full simulation 120 s after ignition. The colors on the horizontal plane indicate bulk ground fuel density, with black being no fuel and bright green being 1 kg/m^3 (0.7 m tall grass). The brown areas are locations where there is less grass, but some fuel litter. The dark green isosurfaces show the tree locations, and the black isosurfaces show parts of the canopy that have been significantly burned. The orange, red, and grey isosurfaces indicate regions of hot gases.

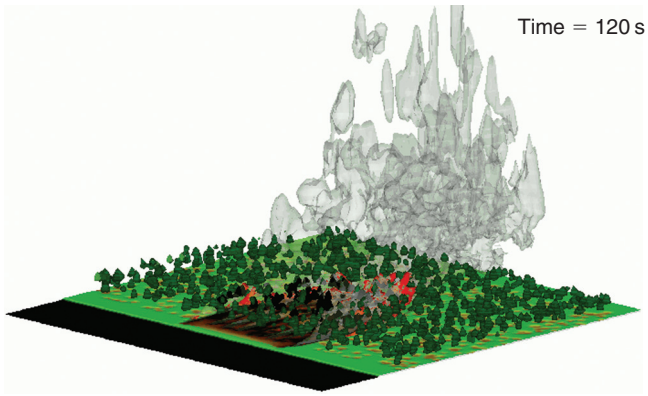

Fig. 4. Image from the thin simulation 120 s after ignition. The colors in this image are similar to those in Fig. 3.

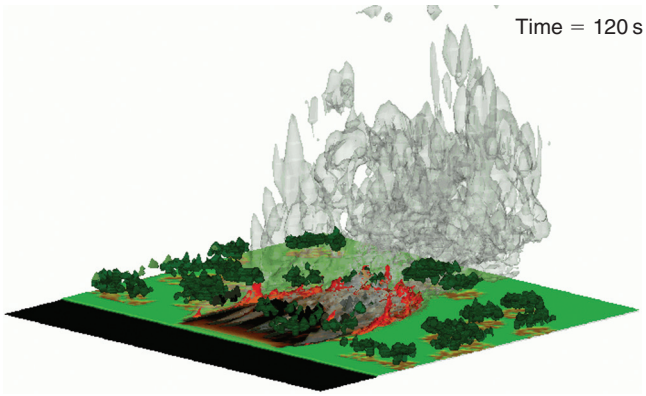

Fig. 5. Image from the patches simulation 120 s after ignition. The colors in this image are similar to those in Fig. 3.

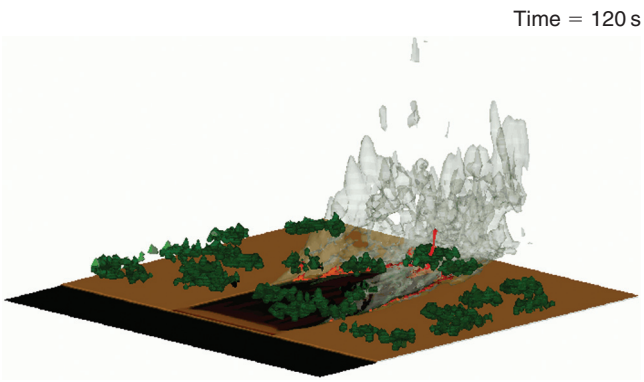

Fig. 6. Image from the patches, less ground fuel (PLGF) simulation 120 s after ignition. The colors on the horizontal plane indicate bulk ground fuel density, with black being no fuel and brown being short grass and litter. The dark green isosurfaces show the tree locations, and the black isosurfaces show parts of the canopy that have been significantly burned. The orange, red, and grey isosurfaces indicate regions of hot gases.

Results and discussion

The reason for performing the four simulations described in the previous section is to provide a basis to demonstrate that HIGRAD/FIRETEC can be used to examine the effects of vegetation structure on fire behavior. Currently, we are examining these properties by comparing magnitudes and qualitatively correlating the evolution of various properties with each other. In the future, we hope to be able to compare these types of simulations to data from real crown fires. One facet of fire behavior that is easily compared between simulations is the distance that the fire front travels, also known as the spread rate.

Figure 7 shows the downwind propagation distances of the fire from the ignition point. From the data shown in this

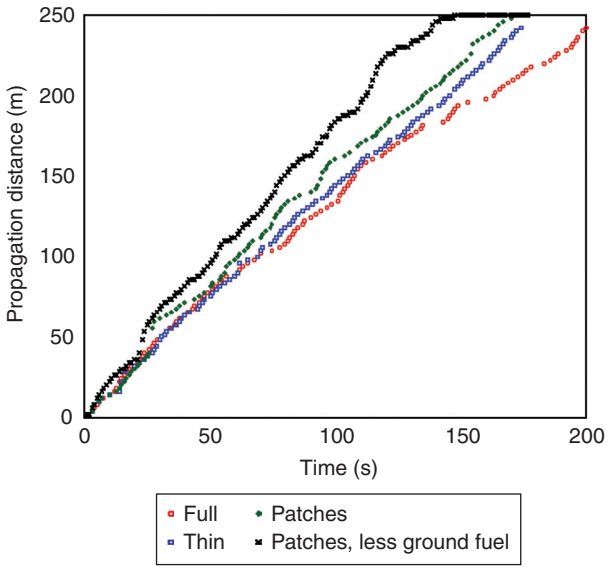

Fig. 7. This figure shows the downwind propagation of the fire front for the four simulations.

Table 1. Summary of the four simulations performed as a part of this study
PLGF, patches, less ground fuel

Simulation	Bulk canopy density (bulk grass density) (kg/m^3)	Canopy description
Full forest	0.24 (0.464)	A canopy that was produced by assembling adjacent 20 m × 50 m regions of trees. Each of these 20 m × 50 m regions includes 81 randomly arranged trees of different shapes and sizes resembling those in a set of data that was measured on a 20 m × 50 m plot near Flagstaff, Arizona.
Thin	0.055 (0.464)	A canopy produced by removing all trees with a trunk diameter at breast height (dbh) less than 28 cm from the canopy used in the full forest simulation.
Patches	0.066 (0.464)	A canopy produced by thinning trees from the canopy used in the full forest simulation to leave patches of uneven-sized trees with spaces in between.
PLGF	0.066 (0.232)	Same as patches, but the grass bulk density has been cut in half.

figure, it is possible to calculate the average rate of spread (slope of the lines shown) of the fires in each simulation. The spread rates range from 1.17 m/s for the full forest simulation to 1.52 m/s for the PLGF simulation. The thin and patches simulations produced mean spread rates of ~1.47 m/s and 1.44 m/s respectively. The spread rates of the fires in the simulations with similar ground fuels are grouped closely, while the spread of the fire in the lighter grasses is faster. This indicates that, under this specific range of conditions, the ground fuel density plays a critical role in determining the overall spread rate even when the fire is burning the canopy. It is commonly observed in real fires that if the crown fire outpaces the ground fire, it will stall and 'wait' for the ground fire to catch up. This is consistent with the overall spread rate of a fire being determined by the ground fuel density and composition. We intend to investigate the reason for this apparent lack of sensitivity of the spread rate to canopy structure in future research.

The spread rate of the fires in these simulations is heavily influenced by the wind that blows through the canopy, understory grasses and stem space. Figure 8 shows average vertical profiles of downwind velocity from a 6000 m^2 domain within the forested regions in the four simulations. These plots contain data derived from spatial averages at an instant in time 6 s after the beginning of the simulations. This particular time was chosen because the winds had had a chance to adjust from the initial uniform wind conditions to reflect the drag caused by the vegetation, but the fire was not yet strongly influencing the flow. The purpose of this figure is to show the average vertical wind shear present in the different fuel distributions in the absence of fire, which is a major difference between the simulations. Once the fire is active in the simulation it dominates many aspects of the wind field (including the average vertical wind shear) and, due to its dynamic nature in our non-steady-state simulation, there is no average state to be discussed. Other aspects of canopy dynamics such as rotational flow are also captured in our simulations (as can be seen in Fig. 9, representing 80 s into a simulation) but are not intended to be illuminated by Fig. 8.

The four plots in Fig. 8 are associated with the full forest, thin, patches and PLGF simulations, and show average downwind velocities for various heights above the ground. In addition, the plots show the mean velocity plus average positive fluctuations and mean velocity less the average negative fluctuations at various heights. The average positive fluctuation is the mean value of all the fluctuations that are greater than zero, and the average negative fluctuation is the mean value of all the fluctuations that are less than zero. These two quantities convey the magnitude of the individual fluctuations above and below the mean, and help differentiate between instances where there are a few large positive or negative fluctuations as opposed to many smaller fluctuations. An example of this can be seen in plots (*c*) and (*d*) of Fig. 8, where the negative velocity fluctuations are much greater than the positive fluctuations in the middle of the overstory fuel layer. We can infer from these values that there are a greater number of positive fluctuations than negative fluctuations. Each of the plots in Fig. 8 also shows the mean bulk fuel density at different heights (measured against the axis on the top of the plots), as well as the mean density plus the average positive density fluctuations and the mean density less the average negative density fluctuations.

The impact of the canopy and understory drag on the winds can be seen by comparing the bulk density values and the average velocities. In all of the plots, the velocity profiles show effects of the canopy, stem space and ground fuel. The stem space velocities, which are nearly the same magnitude as the velocities above the overstory, result from the fact that there are virtually no ladder fuels, the drag of the tree trunks is not accounted for (we are currently working on including this effect), and the sampling area is within 60 m of the leading edge of the forest. At the leading edge of the canopy the flow separates and produces increased velocities above and below the canopy. Because there are no ladder fuels to damp the flow through the stem space, the air funnels into the stem space and is only slowed as the drag effects from the ground fuel and overstory diffuse into the jet of air in the stem space. We would expect the stem space velocities to be less if we had some ladder fuels (even just at the leading edge of the forest) or if we were sampling much farther downwind in the canopy.

When we compare the four plots in Fig. 8, the mean velocities inside the canopy of the full forest simulation are the lowest of the four simulations. The mean velocities of the thin simulation are lower than those of both patches simulations, even though the mean bulk densities are comparable. This difference results from the fact that the scattered large trees in the thin simulation do not provide channels as large as those found between the tree clusters in the patches and PLGF simulations. Also, the scattered nature of the trees in the thin simulation allows the moving air to feel a drag effect from each tree represented, whereas in the patches simulations the clustered nature of the trees shelters some of the trees from the wind. Those sheltered trees therefore do not provide as much drag to the overall flow. The average negative fluctuations in the patches and PLGF simulations are large compared to those of the other simulations. This is, again, because the wind can find channels to quickly move through (shown in Fig. 9), but the clusters form significant obstacles that redirect the wind and limit the flow within them. This also explains why the mean velocity plus the average positive fluctuation is nearly as large as the velocity above the canopy.

The average positive and negative fluctuations are of similar magnitude in the full and thin simulations. This is due to the relatively homogeneous spatial distribution of the trees in these simulations. The lower magnitude of the fluctuations in the full simulation as compared to the thin simulation reflects that the spaces between trees in the full simulation are smaller and the canopy acts more like a continuous

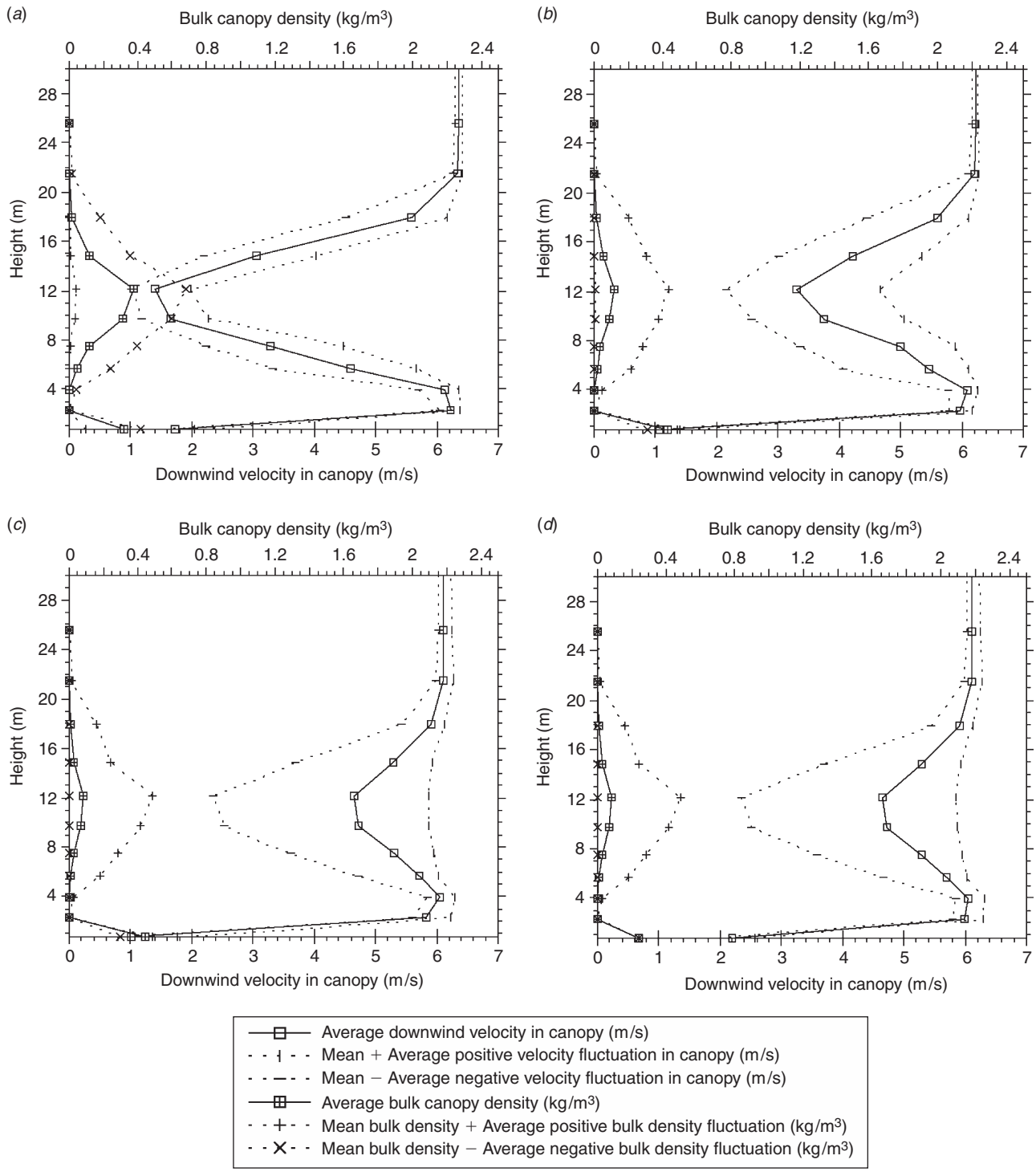

Fig. 8. These four plots associated with the full (*a*), thin (*b*), patches (*c*) and patches, less ground fuel (*d*) simulations show vertical profiles of average downwind velocities and bulk vegetation densities 6 s after the beginning of the simulations. The plots also show the mean values plus the average positive fluctuations and the mean values minus the average negative fluctuations for the velocities and densities.

homogeneous porous medium, which provides a spatially homogeneous drag. The average bulk ground fuel densities shown in Fig. 8 are of similar magnitude in all of the simulations except PLGF, which is half that found in the patches simulation. As a result, the average velocity in the grass layer in the PLGF simulation is more than double the average velocity in the grass layer in the patches simulation as seen in Fig. 8*c*,*d*. The grass layer velocity in the full simulation is

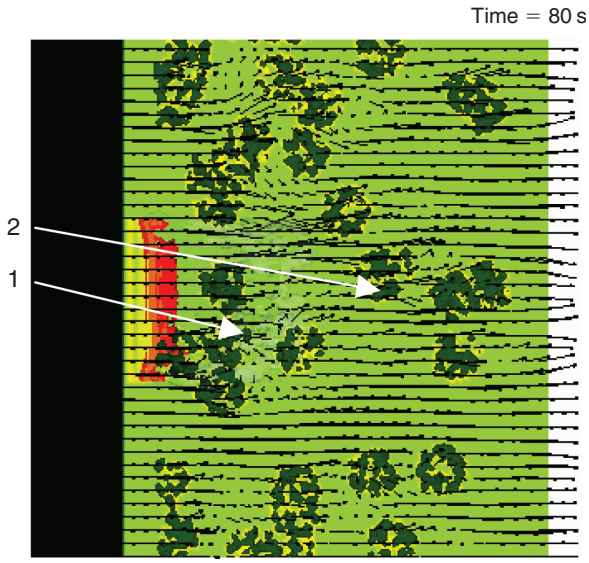

Fig. 9. This image, from the patches simulation, uses vectors to show the flow field 12 m from the ground. The ambient winds at the upper and lower left corners of the image are 6 m/s. The white arrows indicate the two points (trees) that are referred to in the text. The black region is an area where there is no fuel, and the light green areas are the locations of the tall grass. The dark regions are isosurfaces of trees.

significantly larger than in the thin simulation, even though the bulk ground layer vegetation densities are similar. This difference reflects the fact that the full simulation has more litter and less grass than the thin simulation. Thus, the average relative compactness of the ground fuel is greater in the full simulation and causes less drag.

In order to examine the impact of tree arrangement on fire behavior with regard to specific trees, two identical trees at two different specific locations in each of the simulations were chosen. By selecting two identical trees that exist in the same two locations in all four simulations, the impact of location within a non-homogeneous canopy and the impact of various average canopy structures on the way a fire will burn particular trees can be investigated. The trees that were selected have a trunk diameter (at breast height) of 29.4 cm, with a crown radius of 2.75 m. The height of the selected trees is 14.1 m, and the height to live crown is 8.5 m. The locations of these trees are shown in Fig. 9, which is a representation of the patches simulation. The exact same locations were used in the other three simulations, though the trees around them are different in the full forest and thin simulations.

A specific location ~12 m from the ground was chosen in these trees, and the evolution of various characteristics of the fuel, wind and energy transfer at these points is shown in Figs 10–13. The purpose of these figures is to explore and demonstrate the types of information that HIGRAD/FIRETEC can provide, and to incite curiosity about the potential questions that could be addressed with tools such as HIGRAD/FIRETEC. They are meant to show trends and illustrate interesting differences in the fire–atmosphere–fuel interaction with different canopy structures and at different locations within the canopy, not to show details.

The two graphs in Fig. 10 show the mass loss of the vegetation as a function of time. Each of the graphs is associated with one of the two selected points, and contains eight different sets of data values with interpolated curves drawn through them. These curves show the reduction of bulk density of the wood and the reduction of the water from the vegetation as determined by the mixing-limited burning model and moisture evaporation models in FIRETEC. These plots are included to show the evolution of the wood and water quantities as well as the extent of their depletion at the two locations. In both plots, we can see that the water begins to leave the vegetation at a faster rate than the wood. In the full simulation at point 1, and in the full, thin and patches simulations at point 2, the water is driven out completely. Approximately 60% of the wood mass is lost from the full forest at points 1 and 2, and ~65% in the thin forest. There is less than 20% of the wood lost from either of the points in the patches and PLGF simulations.

The two plots in Fig. 11 show the solid (for this purpose, 'solid' includes wood and liquid water) temperature as functions of time. The vegetation at point 1 in the full forest is able to begin burning actively. The temperature reaches nearly 1200 K and remains above 1000 K for approximately 20 s. The temperatures at point 1 in the other simulations never get above 400 K. The temperatures at point 1 in the two patches simulations rise and fall off slowly, while the temperature at point 1 in the thin simulation oscillates at a higher frequency. This oscillation in temperature is believed to be associated with wind oscillations. The temperatures at point 2 in the thin and full forest simulations indicate active burning as they reach temperatures of nearly 1100 K and 1000 K respectively. Point 2 in the patches simulation has a rise in temperature to approximately 475 K, then a decline in temperature and finally a second small rise and fall (peaking at ~350 K). The temperature at point 2 in the PLGF simulation grows slowly to approximately 400 K and declines slowly. These observations are consistent with the trends seen in Fig. 10.

The graphs in Fig. 12 show the bulk convective heating rates as a function of time. In the full simulation at point 1, there is a strong heating period associated with the hot plume being driven over the cooler vegetation, and then a strong cooling period associated with cooler ambient winds being driven over the burning tree after it is ignited. There are smaller amplitude heating and cooling periods for point 1 in the other simulations. The convective heating at point 2 in the PLGF simulation precedes the heating in the other simulations because the ground fire reaches this location faster, as seen in Fig. 7. The convective heating of the vegetation at point 2 in all of the simulations is less than in the full case at point 1. This is probably due to the fact that the temperature

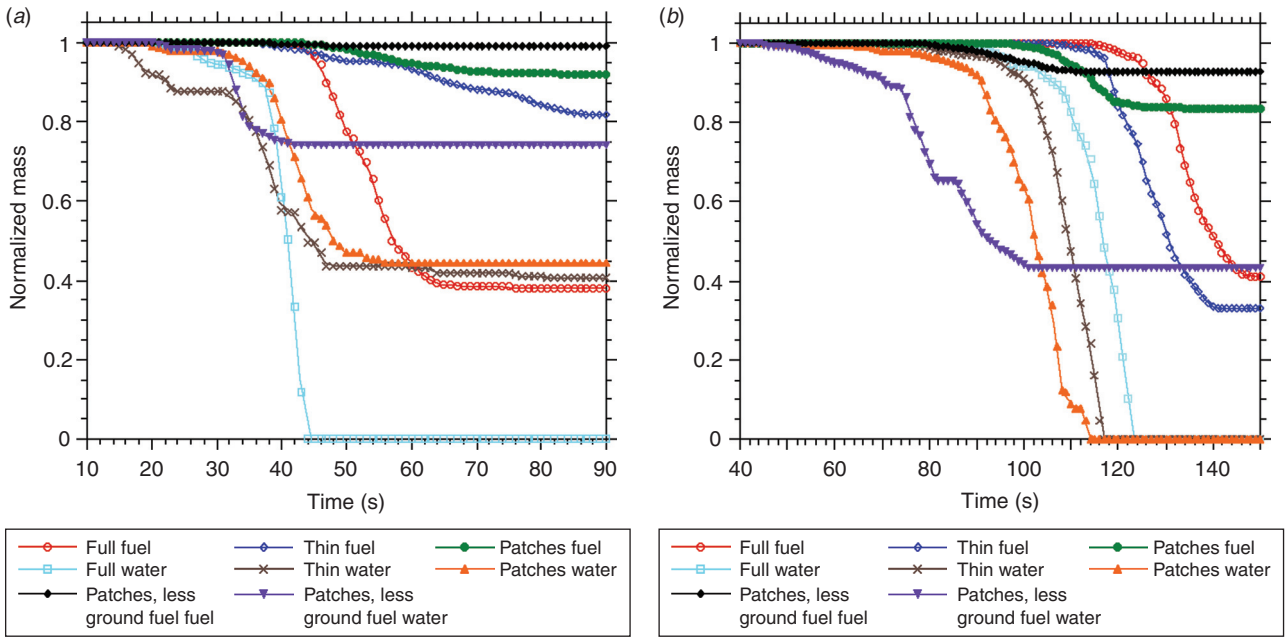

Fig. 10. Plots of vegetation mass loss at points 1 (*a*) and 2 (*b*) as a function of time since ignition.

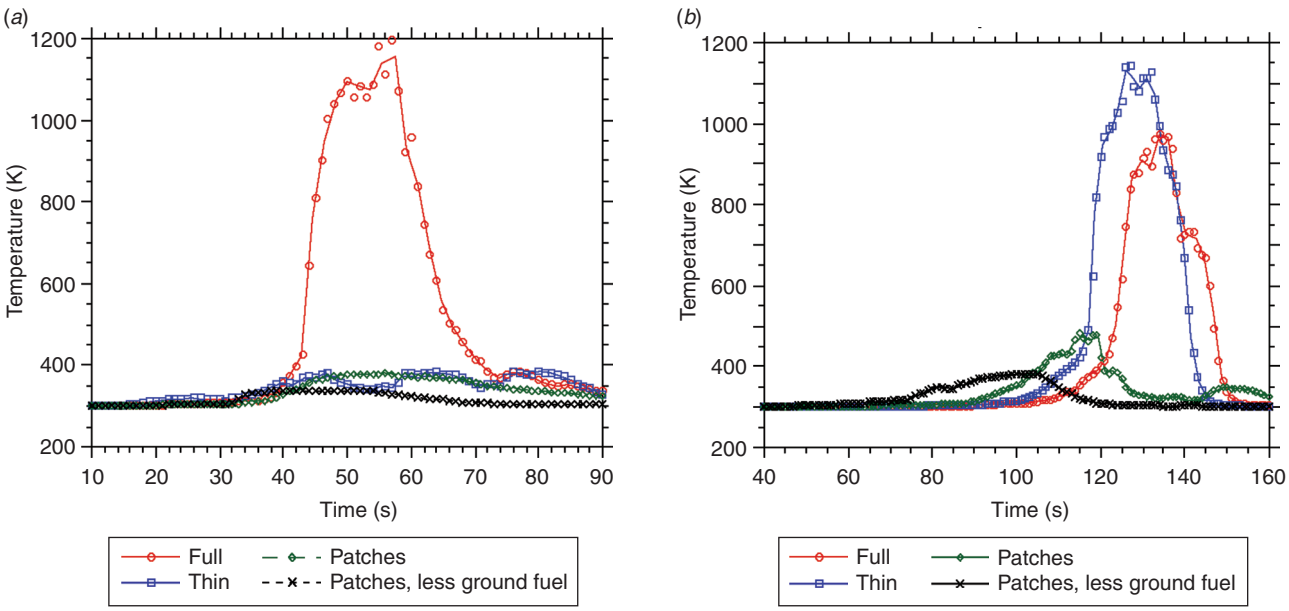

Fig. 11. Plots of the solid temperature at points 1 (*a*) and 2 (*b*) as a function of time since ignition.

of the solid rises at nearly the same rate as the air around it. In these simulations, as the plumes from the ground fires pass by point 2 and the cooler ambient air blows on the vegetation, there is a strong convective cooling effect. This contributes to the incomplete burning in the full and thin simulations (seen in Fig. 10) and the intermediate cooling in the patches simulation (seen in Fig. 11).

The final figure, Fig. 13, shows the net bulk radiative heating rate of the solid as a function of time. In this text, the net bulk radiative heating rate is defined as the energy absorbed by the solid from thermal radiation minus the thermal radiation that is emitted by the solid. The peak heating rate at point 1 in the thin simulation is significantly smaller than the rates for the other simulations at this point. This difference can be attributed to the fact that the trees in the thin simulation are much more dispersed, and so do not have as much radiative heating contribution to each other. The heating rate increases at point 1 faster than it falls off. This indicates that the ground

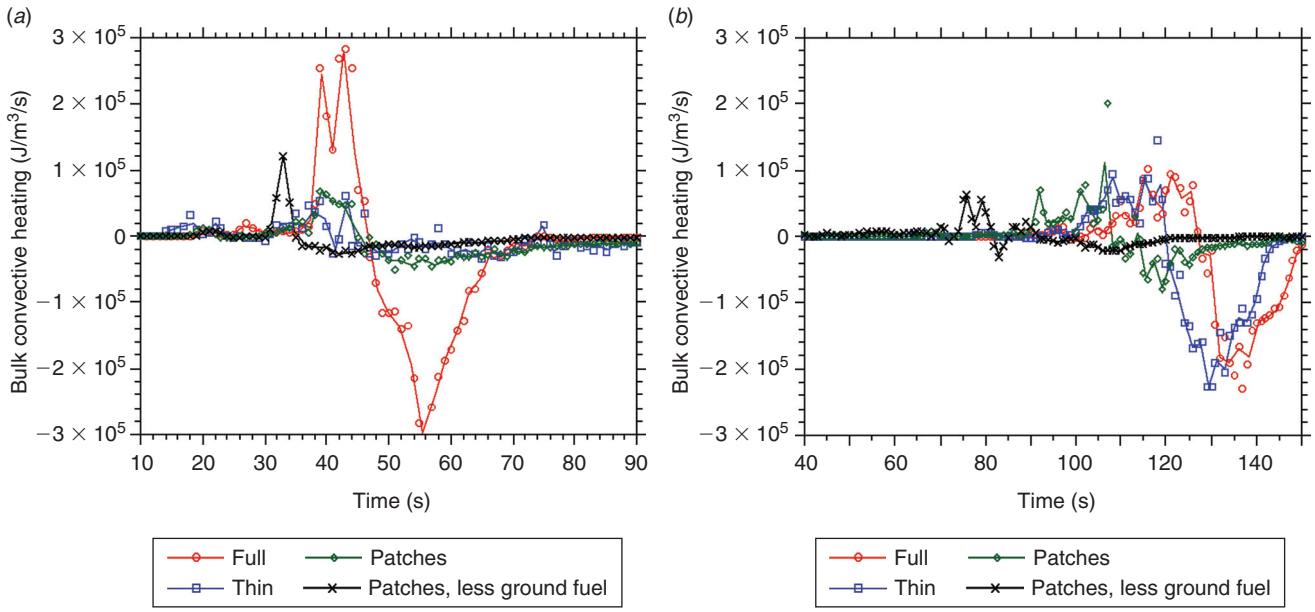

Fig. 12. Plots of the bulk convective heating rate of the solid at points 1 (*a*) and 2 (*b*) as a function of time since ignition.

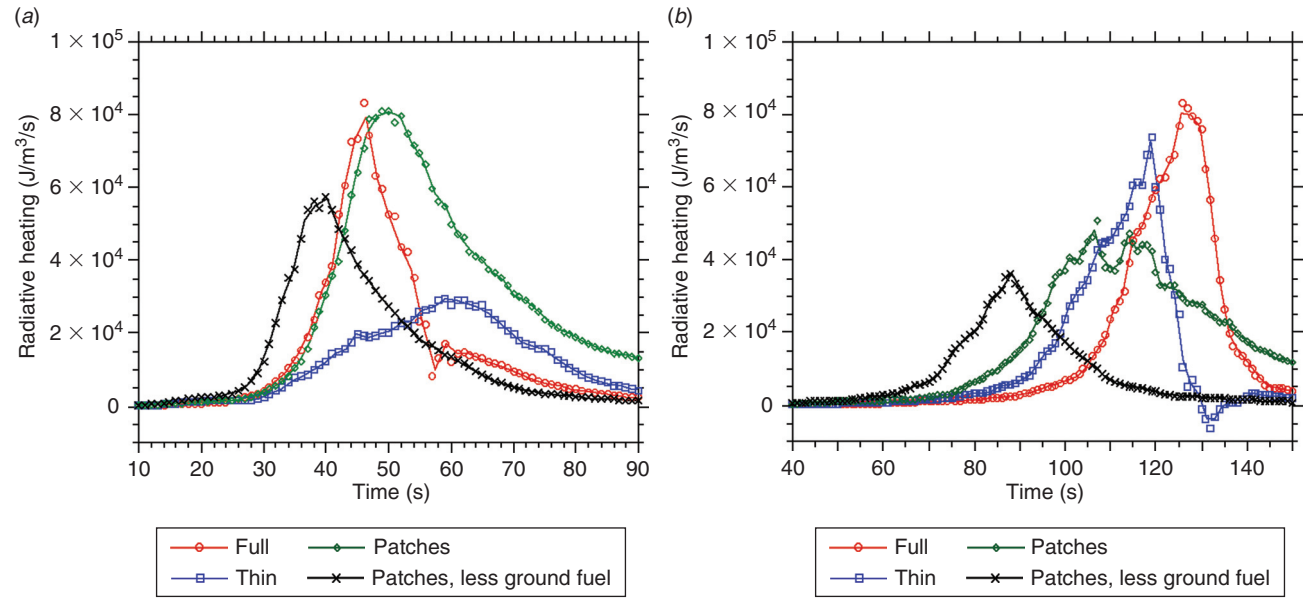

Fig. 13. Plots of the bulk radiative heating rate of the solid at points 1 (*a*) and 2 (*b*) as a function of time since ignition.

fires are still increasing in intensity as they approach point 1 but are fully developed at point 2. Another contributing factor could be that the increase in the heating rate is controlled solely by the movement of the fire front whereas the decrease in the radiative heating rate also depends on the slower rate at which the fuels under point 1 cool down or burn out. The net bulk radiative heating rate in the full case at point 2 is similar in magnitude to that at point 1. The heating rate in the thin simulation at point 2 is much higher than at point 1. In this simulation more trees were ignited around point 2 than around point 1, and so the effect of having the trees dispersed was lessened. The reduction in the radiative heating rate for the two patchy simulations at point 2 could be due to the fact that there are no trees just upwind of the patch of trees where point 2 is located, and so the majority of the trees in the patch itself do not burn significantly. This reduces the tree-to-tree radiation effects. An additional interesting feature shown in Fig. 13 is the negative values in the thin simulation radiative heating rates at point 2. These values are associated with the fact that the solid temperature at point 2 is high, even after

the ground fire has passed. As a result, the tree is actually radiating more energy than it is receiving for a short period of time (potentially igniting other trees). These qualitative descriptions show the effects of different canopy structures on fire behavior. Any one of these examples could be fleshed out in a further series of simulations.

Conclusion

The results described in the previous section illustrate one way that HIGRAD/FIRETEC can be used to compare macroscopic fire behavior (such as propagation distance and spread rate) within different vegetation stands. HIGRAD/FIRETEC was also used to investigate the impact of position or arrangement of individual trees on the chance of a particular tree burning. The simulations provide an illustration of the interaction between the physical processes that drive wildfires and the evolution of the vegetation itself.

The comparison of the PLGF simulation to the patches and other simulations shows that, under some conditions, it is the density of the ground fuel that determines the overall spread rate of the fire even when the overstory is involved in the fire. This might only be true for a select range of wind conditions or canopy densities, so future research will focus on determining under what envelope of conditions this is true.

The simulations show that the position of a tree and the arrangement of the trees around it influence whether that tree will burn or not. By looking at the reported results for the vegetation at point 1 we can see the manner in which the evolution of the physical properties of the vegetation (bulk density, moisture content and temperature) are related to the convective and radiative heating for the various simulations. Clearly, the canopy structure had a significant effect on the significance of the convective heating at point 1 but less effect on the radiative heating. In the full forest simulation the peak convective heating rate is significantly greater than the peak radiative heating rate, whereas the peak radiative and convective heating rates in the other simulations are much more comparable. The more significant convective heating in the full forest case seems to have resulted in the active burning at point 1, which was not present in the other simulations. This is consistent with the idea that the heat is being carried vertically from the ground fire to the canopy, and the effect of the horizontal flow at point 1 is to cool the crown vegetation. In the full forest at point 1, the reduced horizontal winds in the canopy (shown in Fig. 8*a*) allow for the buoyancy-driven vertical winds to be stronger and concentrate more heat. In the other canopy structures, the increased horizontal wind allows for more entrainment of cool air into the rising air and dampens the convective heating of the crown vegetation.

At point 2, the peak convective and radiative heating rates are comparable in all of the simulations. The convective heating rate in the full forest simulation at point 2 is much lower that at point 1. This is due to a combination of events including the reduction of upwind canopy fuels allowing more horizontal wind to reach point 2. Another factor is the longer period of radiative preheating that occurs at point 2 because of the additional radiative contributions of the trees that are already burning. The longer duration of radiative preheating reduces the temperature difference between the solid vegetation and the hot air when it reaches point 2. The comparison of the contribution of convective heating at point 1 and point 2 shows that there are different heat transfer balances occurring at different times and different locations, especially with regard to fires in non-uniform fuel beds such as those being simulated. In fact, this type of study could shed additional insight into the difference between the processes that sustain an existing crown fire as opposed to those required for the transition from a ground fire to a crown fire (point 2 *v.* point 1).

Another significant difference is the active burning at point 2 in the thin simulation, which is not present at point 1. This difference appears to be tied to the higher rate of radiation heat transfer at point 2. This larger rate has been attributed to the additional strength in the ground fire as well as additional trees on fire near point 2. Any increase in the number of radiation sources can impact point 2 in the thin simulation more strongly then it does in the full forest simulation because of the longer effective optical path lengths in the thin canopy. There are fewer trees to shield the radiation from reaching point 2. In the patches simulation the radiative heating begins sooner because there is a wide unobscured space upwind of point 2, but the peak radiative-heating rate is smaller because there are no burning trees just upwind of point 2. This result shows the combined impact of the location with respect to the ignition point and the bulk and local properties of the canopy.

These are a few of the observations and bits of qualitative insight that can be gained from this set of four simulations. Without a significant amount of validation and comparison with experiments, it is very premature to put emphasis on the actual values produced by these types of simulations. They do, however, provide a valuable tool for looking at the interactions between the physical processes that influence wildfires and the fire's behavior. With sufficient validation, they could eventually play a roll in helping managers to decide between different thinning and fuel treatment strategies at specific locations.

Summary

In this text, we have introduced the use of HIGRAD/FIRETEC for simulating fires as they move through forests made of individual treelike fuel elements. There are many ways to approximate the distribution of ground fuels under the canopies. We chose a simplified algorithm for this text but anticipate the inclusion of more sophisticated algorithms in the future. We hope to draw on the experience of Forest Service researchers to help inform the development of this

algorithm. HIGRAD/FIRETEC is not a high fidelity combustion model, and does not attempt to capture the details of the combustion process or the fine-scale details of the vegetation. HIGRAD/FIRETEC does, however, model the physics of many of the important processes that drive a wildfire, and captures many of the complex interactions between fire, atmosphere and fuel.

To illustrate the use of this model for simulating forest canopies, we chose two different trees that each existed identically in four different simulations. By examining a set of characteristics of the atmosphere and solid fuel at a location 12 m above the ground in each of these trees in the various simulations, we can see indications of different phenomena occurring as a result of a tree's location with respect to the ignition point, other trees, and the understory vegetation.

The number of simulations presented here is not sufficient to provide conclusive results about all of the interdependencies that occur in the simulations, but they are sufficient to inspire many new questions and to guide future research directions.

In order for information from this type of model to be of true value, we must find ways to compare the results with experiments and real fires. By making these comparisons, we can gain confidence in the aspects of the model that are working correctly and obtain critical information about the deficiencies of the model that need improvement. By recognizing differences between the model and real fire behavior, researchers will learn more about the interaction between the driving processes in wildfires.

References

Albini FA, Stocks BJ (1986) Predicted and observed rates of spread of crown fires in immature jack pine. *Combustion Science and Technology* **48**, 65–76.

Belcher SE, Jerram N, Hunt JCR (2003) Adjustment of a turbulent boundary layer to a canopy of roughness elements. *Journal of Fluid Mechanics* **488**, 369–398. doi:10.1017/S0022112003005019

Brunet Y, Finnigan JJ, Raupach MR (1994) Wind tunnel study of air flow in waving wheat: single-point velocity statistics. *Boundary-Layer Meteorology* **70**, 95–132. doi:10.1007/BF00712525

Call PT, Albini FA (1997) Aerial and surface fuel consumption in crown fires. *International Journal of Wildland Fire* **7**, 259–264.

Calogine D, Sèro-Guillaume O (2002) Air flow model in a tree crown. In 'Proceedings of the fourth international conference on forest fire research', November 2002, Luso, Coimbra, Portugal. (CD-ROM) (Millpress: Rotterdam)

Cruz MG, Alexander ME, Wakimoto RH (2002) Predicting crown fire behavior to support forest fire management decision-making. In 'Proceedings of the fourth international conference on forest fire research', November 2002, Luso, Coimbra, Portugal. (CD-ROM) (Millpress: Rotterdam)

Finnigan JJ, Brunet Y (1995) Turbulent air flow in forests on flat and hilly terrain. In 'Wind and trees'. (Eds MP Coutts, J Grace) pp. 3–7. (Cambridge University Press: Cambridge)

Linn RR (1997) 'Transport model for prediction of wildfire behavior.' Los Alamos National Laboratory Scientific Report: LA13334-T. (Los Alamos National Laboratory: Los Alamos, NM)

Linn R, Reisner J, Colman JJ, Winterkamp J (2002) Studying wildfire using FIRETEC. *International Journal of Wildland Fire* **11**, 1–14.

Morvan D, Dupuy JL (2001) Modeling of fire spread through a forest fuel bed using a multiphase formulation. *Combustion and Flame* **127**, 1981–1994. doi:10.1016/S0010-2180(01)00302-9

Reisner J, Swynne S, Margolin L, Linn R (2000*a*) Coupled atmospheric–fire modeling employing the method of averages. *Monthly Weather Review* **128**, 3683–3691. doi:10.1175/1520-0493(2001)129<3683:CAFMET>2.0.CO;2

Reisner J, Knoll DA, Mousseau VA, Linn R (2000*b*) New numerical approaches for coupled atmosphere-fire models. In 'Third symposium on fire and forest meteorology'. January 2000, Long Beach, CA. pp. 11–13. (American Meteorology Society: Boston, MA)

Rothermel RC (1991) Predicting behavior and size of crown fires in the northern Rocky Mountains. USDA Forest Service, Intermountain Research Station Technical Report INT-438. (Ogden, UT)

Shaw RH, Brunet Y, Finnigan JJ, Raupach MR (1995) A wind tunnel study of air flow in waving wheat: two-point velocity statistics. *Boundary-Layer Meteorology* **76**, 349–376. doi:10.1007/BF00709238

Van Wagner CE (1993) Prediction of crown fire behavior in two stands of jack pine. *Canadian Journal of Forest Research* **23**, 442–449.